



Contents lists available at ScienceDirect

Biochemical and Biophysical Research Communications

journal homepage: www.elsevier.com/locate/ybbrc

HGF/SF and menthol increase human glioblastoma cell calcium and migration

Robert Wondergem^{a,*}, Tom W. Ecay^a, Frank Mahieu^c, Grzegorz Owsianik^b, Bernd Nilius^b

^a Department of Physiology, James H. Quillen College of Medicine, East Tennessee State University, P.O. Box 70,576, Johnson City, TN 37614-1708, USA

^b Department of Molecular Cell Biology, Division of Physiology, Laboratory of Ion Channel Research, Katholieke Universiteit, B-3000 Leuven, Belgium

^c GROEP T—Leuven Engineering College, Associatie Katholieke Universiteit, Vesaliusstraat 13, B-3000 Leuven, Belgium

ARTICLE INFO

Article history:

Received 30 April 2008

Available online xxxx

Keywords:

Transient receptor potential ion channel TRPM8

Hepatocyte growth factor/scatter factor

HGF/SF

DBTRG

Migration

Glioblastoma

Calcium

ABSTRACT

This study explored the role of transient receptor potential melastatin 8 ion channels (TRPM8) in mechanisms of human glioblastoma (DBTRG) cell migration. Menthol stimulated influx of Ca^{2+} , membrane current, and migration of DBTRG cells. Effects on Ca^{2+} and migration were enhanced by pre-treatment with hepatocyte growth factor/scatter factor (HGF/SF). Effects on Ca^{2+} also were greater in migrating cells compared with non-migrating cells. 2-Aminoethoxydiphenyl borate (2-APB) inhibited all menthol stimulations. RT-PCR and immunoblot analysis showed that DBTRG cells expressed both mRNA and protein for TRPM8 ion channels. Two proteins were evident: one (130–140 kDa) in a plasma membrane-enriched fraction, and a variant (95–100 kDa) in microsome- and plasma membrane-enriched fractions. Thus, TRPM8 plays a role in mechanisms that increase $[\text{Ca}^{2+}]_i$ needed for DBTRG cell migration.

© 2008 Elsevier Inc. All rights reserved.

Glioblastoma multiforme (GBM) has a particularly grim prognosis. The extreme invasive property of this tumor, along with propensity of phenotypic changes to occur within the population of invading cells compared with the primary tumor mass, present unyielding dilemmas for effective surgical, chemo- or radiation therapy. Thus, efforts to understand the mechanisms by which tumor cells migrate and invade will provide useful information to alleviate the progression of this disease.

We have set out to identify transient receptor potential ion channels (TRPs) that contribute to mechanisms of cell migration and tumor metastases by virtue of their role in controlling intracellular Ca^{2+} , $[\text{Ca}^{2+}]_i$. We first demonstrated that increased Ca^{2+} influx via TRP vanilloid member 1 and 4 ion channels (TRPV1 and TRPV4) accompanied hepatocyte growth factor/scatter factor (HGF/SF)-stimulated human hepatoblastoma (HepG2) cell migration [1]. Subsequent studies showed that capsaicin (a TRPV1-specific agonist) increases both Ca^{2+} influx and migration in HepG2 cells, but only those treated previously with HGF/SF [2].

HGF/SF is a multifunctional effector of cells expressing the Met tyrosine kinase receptor [3]. HGF/SF-Met binding stimulates cell migration, and it is essential for normal embryological development of tissues [3]. However, the ligand–receptor pair also plays a role in malignancy of many solid tumors [3], including gliomas [4,5].

We now provide evidence of TRP channel involvement in the migration of human GBM (DBTRG) cells. Our findings suggest that, like TRPV1 in HepG2 cells, TRP melastatin member 8 ion channels (TRPM8) activity affect the rate of GBM cell migration, as does HGF/SF stimulation, by controlling the influx of $[\text{Ca}^{2+}]_i$. TRPM8 is highly expressed in prostate and other cancer cells [6], but, apart from its principal function in neurons as a detector of environmental cold [7], its physiological and pathological function in epithelia and cancer cells is unknown [8].

Materials and methods

Cell culture and materials. Human GBM cells (DBTRG cells) and HGF/SF were a gift from G.F. Vande Woude, Van Andel Research Institute, Grand Rapids, MI. Cells were grown in Dulbecco's MEM supplemented with 10% FBS (Invitrogen) and 100 IU–100 $\mu\text{g}/\text{ml}$ penicillin–streptomycin (Sigma).

RNA isolation, cDNA synthesis, and reverse transcriptase PCR. Total RNA was isolated from confluent cultures of DBTRG cells using RNA-Bee (Tel-Test). SuperScript First-Strand Synthesis System (Invitrogen) was used for reverse transcription of 5 μg total RNA. Amplification of TRPV1 and TRPM8 specific sequences was performed with AccuPrime Super Mix 1 (Invitrogen) and gene specific primers (Table 1) designed to match those used successfully in past studies [1,9]. Conditions for amplification were denaturation at 94 °C for 20 s, annealing at 62 °C for 20 s, and extension at 68 °C for 1 min for 35 cycles.

* Corresponding author. Fax: +1 423 439 2052.

E-mail address: wonderge@etsu.edu (R. Wondergem).

Table 1
PCR primers used to probe DBTRG cells for TRPV1 and TRPM8 RNA expression

Gene	Primer		Size of amplicon (bp)
	Forward	Reverse	
TRPV1	CAGCCACCTCAAGGAGTATG	GCCTGAAACTCTGCTTGACC	766
TRPM8 set 1	TGTCGGCTCTTTCTGGAG	CTTATTCTGAAGAATGGCCAG	300
TRPM8 set 2	TGTTTTGCCCAAGGAGGTGG	CAACCAGTTCCAGACAAACG	680

Cell fractionation and immunoblotting. Confluent DBTRG cultures were lysed, homogenized, and fractionated by differential centrifugation as described elsewhere [10]. Protein concentration was determined by BCA assay (Pierce). Equal protein samples were fractionated on 5–15% gradient SDS–PAGE gels and electroblotted to PVDF (Millipore). Blots were blocked, reacted with anti-TRPM8 antibody [9], secondary antibody, and developed by chemiluminescence (Pierce) by methods described elsewhere [11]. To ascertain specific binding TRPM8 antibody (0.5 µg/ml) was preadsorbed to TRPM8 peptide (4 µg/ml) used as antigen [9].

Whole-cell voltage-clamp technique. DBTRG cells were superfused on a microscope stage at room temperature with a standard external salt solution containing (in mM): 150 NaCl, 6 KCl, 1 MgCl₂, 1.5 CaCl₂, 10 Hepes [N-(2-hydroxyethyl)piperazine-N'-(2-ethanesulfonic acid)], 10 glucose, and pH 7.4 (1 N HCl). Whole-cell patch-clamp pipettes (4–5 MΩ in the bath solution) were filled with (in mM): 20 CsCl, 100 aspartic acid, 0.1 CaCl₂, 1 MgCl₂, 5 EGTA 10 Hepes, 4 Na₂ATP, and pH 7.2 (1 N CsOH). Cells were warmed to 37 °C by a thermistor-based controller. Whole-cell voltage-clamp measurements were by standard technique [12].

Ca²⁺ measurements by fluorescence imaging of Fura2. Cells on glass coverslips were loaded with Fura2 and [Ca²⁺]_i was measured by inverted microscopy (AccuScope 3030) [1]. Filter-wheel and data acquisition were controlled by the InCyte2 software (Intracellular Imaging, Inc., Cincinnati). [Ca²⁺]_i was determined by interpolation from a standard curve generated from a Ca²⁺ calibration buffer kit #2 (Molecular Probes) and Fura2/K₅-salt.

Cell migration assay. DBTRG cells are plated into 12-well tissue culture plates and grown until confluent. A disposable pipette tip (250 µL) was used to scratch a wound on midline of the culture well. Photomicrographs were taken at various times, and wound width was measured and recorded using MetaMorph software (Molecular Devices), which was calibrated at µm/pixel by the grid on a hemocytometer.

Data analysis. Results are expressed as means ± SEM. Differences among means were determined by ANOVA and comparisons between individual groups were tested using Student's *t*-test, *p* < 0.05. Migration rates were determined by regression analysis of wound width versus time (h), and treatments were deemed effective compared with control if the null-hypothesis of common slopes ($H_0: b_1 - b_2 = 0$) was rejected at *p* < 0.05.

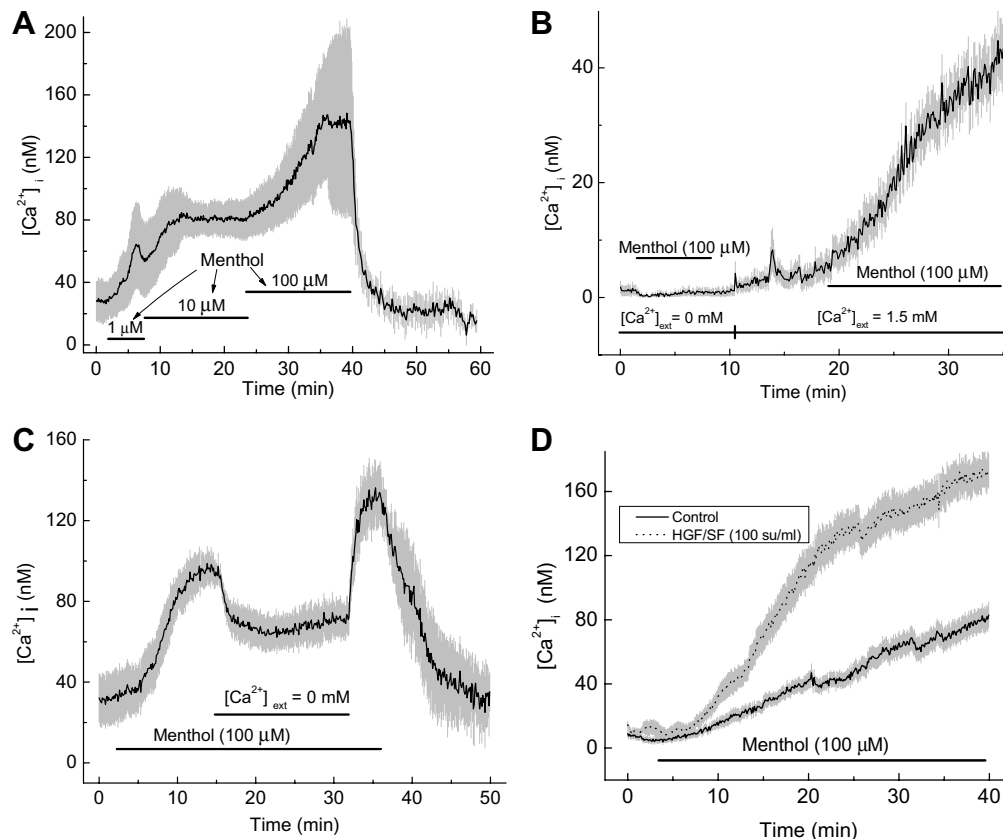


Fig. 1. Effect of menthol on intracellular Ca²⁺, [Ca²⁺]_i, in DBTRG cells measured by Fura2 fluorescence, means ± SE. (A) Effect of increasing dose of menthol on [Ca²⁺]_i, (*n* = 5 of 36 cells). (B) Effect of external Ca²⁺ concentration on menthol stimulation of [Ca²⁺]_i, (*n* = 17 of 38 cells). (C) Effect of reducing external Ca²⁺ concentration to 0 mM following menthol stimulation and increase of [Ca²⁺]_i, (*n* = 15 of 26 cells). (D) Effect of menthol on [Ca²⁺]_i in cells treated for 20-h with HGF/SF compared with untreated control cells (*n* = 36 each group). Temperature = 23 °C.

Results

DBTRG cells secrete autocrine HGF/SF [4]; thus, we postulated that these cells contain heat-sensitive TRP ion channels, TRPV1 and TRPV4, as we had shown in HGF/SF-responsive HepG2 cells [1,2]. Unexpectedly, both capsaicin (not shown) and elevated temperature (below) decreased DBTRG whole-cell membrane current, and added capsaicin also decreased the rate of DBTRG cell migration (not shown), which indicated that GBM cells function differently compared with hepatoblastoma cells.

Since TRPM8 is expressed in other cancers [6], we measured effects of menthol on DBTRG cell Ca^{2+} . Menthol increased $[\text{Ca}^{2+}]_i$ in a dose-dependent manner, albeit in a protracted time-course that took as long as 10 min but reversed on washout, Fig. 1A. Menthol did not increase $[\text{Ca}^{2+}]_i$ when added to external solution with $[\text{Ca}^{2+}]_{\text{ext}} = 0 \text{ mM}$; however, menthol increased $[\text{Ca}^{2+}]_i$ following restoration of $[\text{Ca}^{2+}]_{\text{ext}}$ to 1.5 mM, Fig. 1B. Elimination of external Ca^{2+} during menthol stimulation reduced $[\text{Ca}^{2+}]_i$ but not to pre-stimulated levels, and $[\text{Ca}^{2+}]_i$ increased even more on restoration of external Ca^{2+} , Fig. 1C. This indicated that menthol also affects

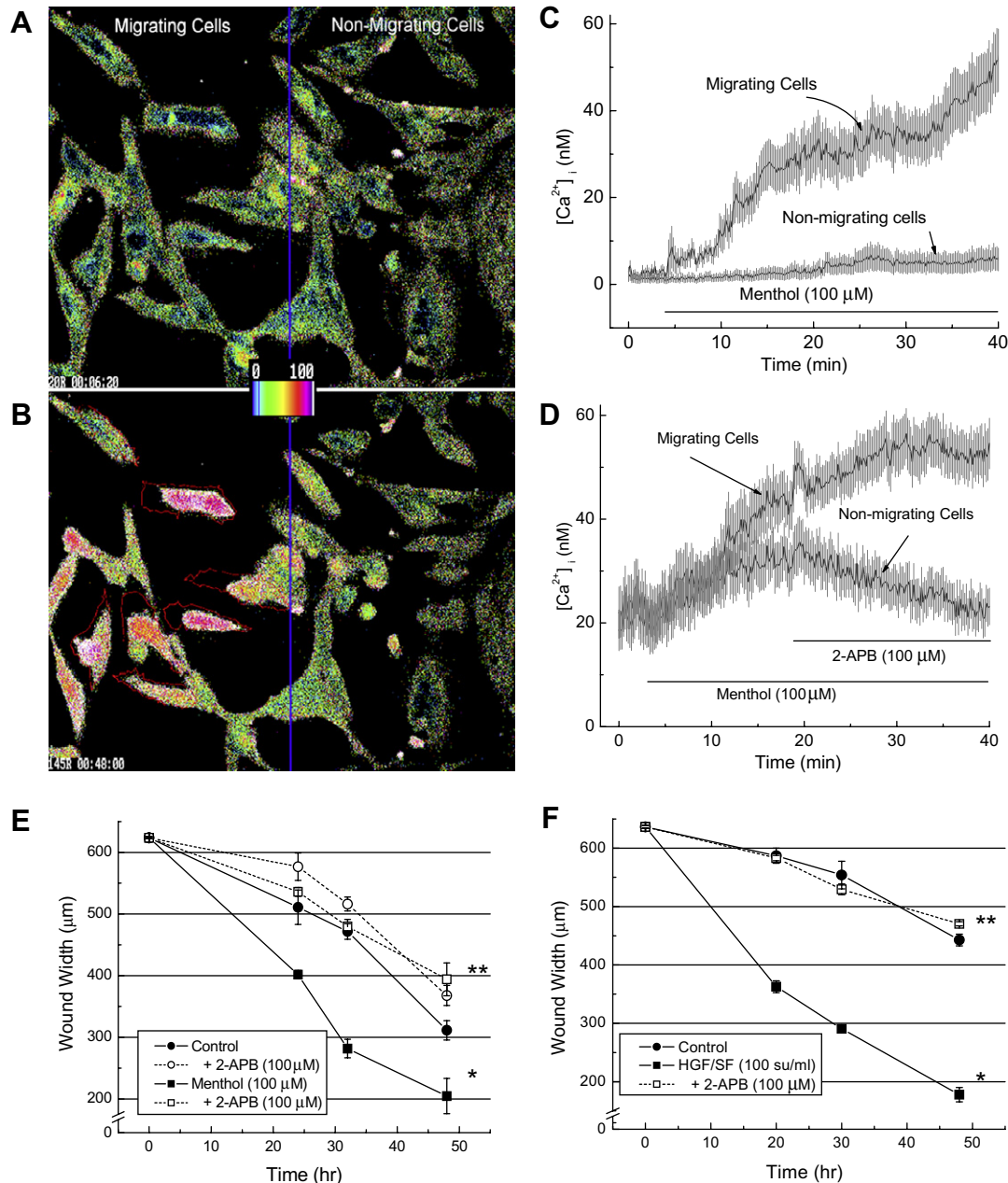


Fig. 2. Effect of menthol on intracellular Ca^{2+} , $[\text{Ca}^{2+}]_i$, in non-migrating (right) and migrating DBTRG cells (left). Cell migrated for 24 h into scratch wounds made in confluent cells. (A) Pseudo-colored Fura2 fluorescence in cells before added menthol. (B) Pseudo-colored Fura2 fluorescence in cells 35 min after added menthol. Red lines are overlays of outlines taken of selected cells at time zero in (A). (C) $[\text{Ca}^{2+}]_i$ versus time after added menthol (100 μM) in non-migrating cells (means \pm SE; $n = 12$) and migrating cells (means \pm SE; $n = 12$). (D) $[\text{Ca}^{2+}]_i$ versus time after added menthol (100 μM) and 2-APB (100 μM) in non-migrating cells (means \pm SE; $n = 12$) and migrating cells (means \pm SE; $n = 12$). Temperature = 23 $^{\circ}\text{C}$. (E,F) DBTRG cell scratch-wound closure versus time (h). (E) Effects of added menthol (100 μM) and 2-aminoethoxydiphenyl borate (2-APB; 100 μM) versus time. **Menthol + 2-APB differs from menthol, $p < 0.01$; menthol differs from control, $p < 0.001$. (E) Effect of added HGF/SF (100 scatterunits/ml) and 2-APB (100 μM) on wound width versus time. **HGF/SF + 2-APB differs from HGF/SF, $p < 0.001$; HGF/SF differs from control, $p < 0.001$. Each point is the mean \pm SEM ($n = 3$). Temperature = 37 $^{\circ}\text{C}$.

Ca^{2+} release from intracellular stores, most likely secondarily by Ca^{2+} -stimulated release since menthol did not increase $[\text{Ca}^{2+}]_i$ in Ca^{2+} -free solution. Nevertheless, effects of menthol on $[\text{Ca}^{2+}]_i$ in DBTRG cells were observed in 14–58% of the cells selected within the microscopic field. $[\text{Ca}^{2+}]_i$ in remaining cells either did not respond to added menthol or it increased exceedingly slowly over 40–60 min.

DBTRG cells autosecrete HGF/SF along with overexpression of c-Met [4], which might account for the differential response of DBTRG cells to added menthol. To test this we compared the effect of menthol on $[\text{Ca}^{2+}]_i$ in HGF/SF-treated (100 scatterunits/ml for 20 h), non-confluent cells compared with untreated control cells. Here, both rate of accumulation and total DBTRG $[\text{Ca}^{2+}]_i$ in response to added menthol (100 μM) was greater in HGF/SF-treated cells compared with untreated cells, Fig. 1D.

HGF/SF stimulated $[\text{Ca}^{2+}]_i$ in migrating HepG2 cells compared with non-migrating cells [1]. Thus, we postulated that such differential menthol responsiveness might be evident between in DBTRG cells since they secrete HGF/SF [4]. So, we grew DBTRG cells to confluence, created scratch wounds and allowed cells to migrate into the wounds for 24 h. We then added menthol and measured $[\text{Ca}^{2+}]_i$ in cells selected from the migrating and non-migrating populations. Fig. 2A shows images pseudo-colored for $[\text{Ca}^{2+}]_i$ of non-migrating cells (right) and migrating cells (left) prior to added menthol. Fig. 2B shows the same cells 40 min following added menthol. Color changes depict menthol-stimulated increase in $[\text{Ca}^{2+}]_i$ in migrating cells compared with non-migrating cells. We also overlaid outlines taken of selected cells at time zero, Fig. 2A, onto Fig. 2B. This shows that cells retracted from their footplate attachments during the rise in $[\text{Ca}^{2+}]_i$ with added menthol. All cells retracted to some degree with added menthol, but retraction was most evident among migrating cells. Time-courses for comparative increases in $[\text{Ca}^{2+}]_i$ by added menthol on both cell samples shows greater responsiveness of migrating cells compared with non-migrating cells, Fig. 2C. We also added 2-APB (100 μM), a purported, albeit non-specific inhibitor of TRPM8 [13], during the course of menthol stimulation. This inhibited menthol-stimulated increases of $[\text{Ca}^{2+}]_i$ but was more evident in non-migrating cells, Fig. 2D.

Menthol (100 μM) also stimulated cell migration as evidenced by increased rate of wound closure compared with un-

treated cells, and 2-APB (100 μM) added concurrently inhibited stimulation by menthol, Fig. 2E. Although constitutively secreted by DBTRG cells [4], added HGF/SF (100 scatterunits/ml) also stimulated cell migration, and rate of wound closure was similar to that by menthol. 2-APB (100 μM) added concurrently with HGF/SF inhibited its stimulation of DBTRG cell migration, Fig. 2F.

To determine whether functional effects of menthol might be attributable to TRPM8 in DBTRG cells, we probed for TRPM8 mRNA and protein in DBTRG, Fig. 3. Two sets of oligonucleotide primers (Table 1) designed to match sequences in human TRPM8 [9] produced single rtPCR amplification products with sizes predicted for expression of TRPM8 mRNA by DBTRG cells, Fig. 3A. An antibody against a conserved C-terminal peptide sequence of human TRPM8 [9] recognized a single major band at 95–100 kDa in homogenates of DBTRG cells, Fig. 3B. This band was not resolved if antibody was preadsorbed to antigenic peptide. When DBTRG crude homogenate was fractionated by centrifugation, both plasma membrane-enriched high-speed pellet and high-speed supernatant fractions (cytosol and microsomes) contained an immunoreactive 95–100 kDa band. However, a fainter band at 130–140 kDa was observed in the lane corresponding to the plasma membrane-enriched high-speed pellet. Again, these bands were not recognized by preadsorbed antibody. Thus, there are two TRPM8 proteins, one in the high-speed pellet/plasma membrane fraction at a size predicted by the cDNA sequence [9,14] and one smaller than predicted resided in both plasma membrane and microsomal fractions.

Whole-cell voltage-clamp measurements showed inwardly- and outwardly-rectifying currents with reversal potentials near zero, Fig. 4B and C. Raising cell temperature eliminated the currents, which returned on cooling, Fig. 4A–C. Membrane currents decreased with heating, which is characteristic of TRPM8, in 8 out of 12 cells.

To test further the presence of TRPM8 ion channels in DBTRG cells we applied menthol during whole-cell recording at 22 °C, Fig. 4D. Inward and outward membrane currents increased within 30–60 s of added menthol (100 μM), Fig. 4D–F. However, the increase in inward current with menthol was unexpected in comparison with TRPM8 activated in heterologous expression systems where membrane cur-

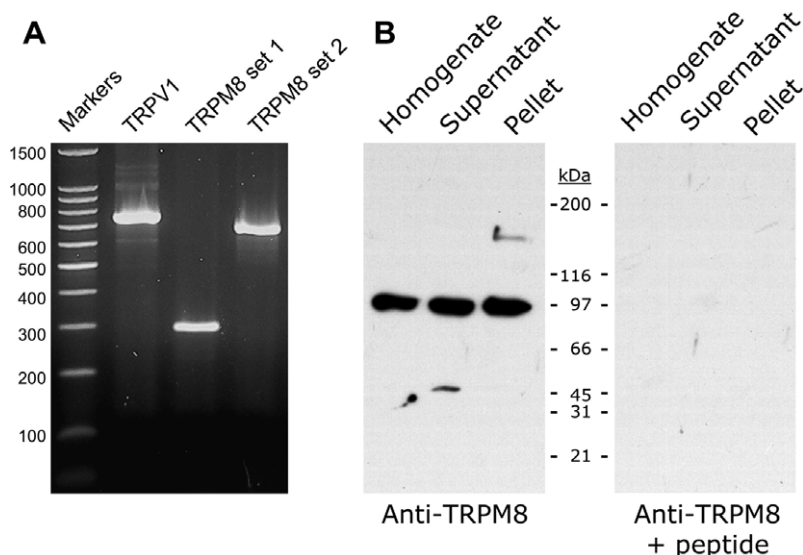


Fig. 3. Molecular identification of TRPM8 expression in DBTRG cells. (A) Agarose gel electrophoresis of PCRs using DBTRG cDNA and the indicated primer sets (Table 1). TRPM8 primers produced a single major product at the expected size for amplification of TRPM8 sequences. (B) Immunodetection of TRPM8 in DBTRG cells. Confluent DBTRG cultures were homogenized (H) and fractionated by centrifugation into high-speed supernatant (S) and pellet (P) fractions. Equal protein samples (50 $\mu\text{g}/\text{lane}$) of each fraction were separated by SDS-PAGE and blotted to PVDF. Identical blots were reacted with either TRPM8 antibody or TRPM8 antibody preadsorbed with blocking peptide.

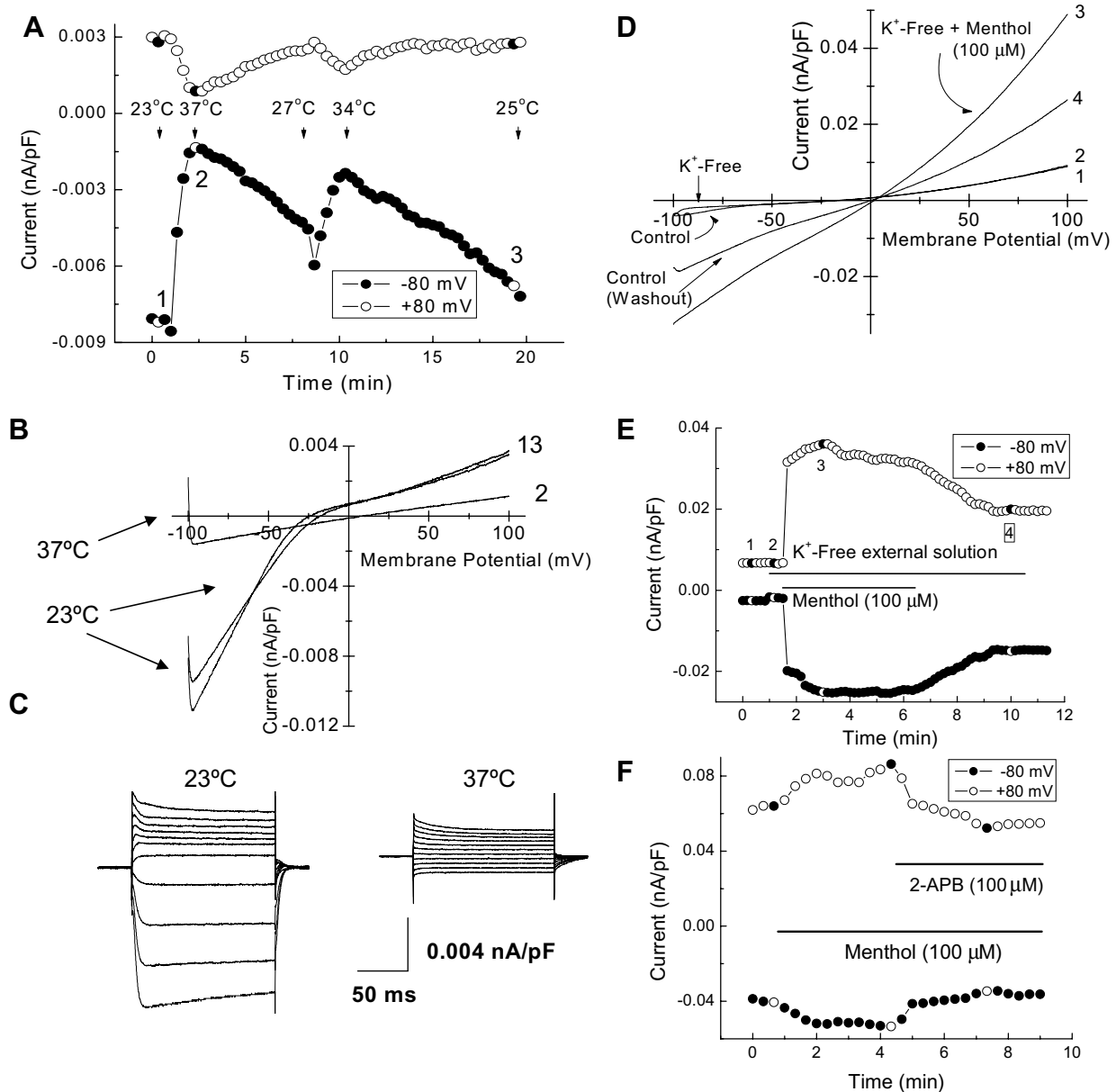


Fig. 4. Whole-cell patch-clamp recordings of DBTRG cells during temperature change and effect of menthol. (A) Time-dependent changes in inward (at -80 mV) and outward (at $+80$ mV) membrane current during heating and cooling between 23 and 37 °C. Numbers indicate currents corresponding to full traces shown in (B). (B) Whole-cell recording showing current-voltage plots at different temperatures. Voltage ramps from -100 to 100 mV were applied over 300 ms at 23 °C, at 37 °C and at 25 °C (restored). (C) Whole-cell recording showing currents from consecutive 20-mV voltage steps (-100 to 100 mV) at different temperatures. (D) I-V plots taken before and after added agents. Numbered traces correspond to numbered outward and inward currents in (E). (E) Effect of added menthol (100 μ M) in a K^+ -free external salt solution on inward (-80 mV) and outward ($+80$ mV) membrane current versus time. Numbered traces correspond to numbered I-V plots in (D). (F) Effect of added menthol (100 μ M) followed by added 2-aminoethoxydiphenyl borate (2-APB; 100 μ M) on inward (-80 mV) and outward ($+80$ mV) membrane current versus time. Temperature = 23 °C for D–F. Holding potential = -30 mV for all measurements.

rent rectifies outwardly [15]. To rule out possible involvement of inward rectifier K^+ currents (K_{ir}), which may not be blocked by Cs^+ within the pipette, we measured effect of menthol following superfusing a solution in which all external K^+ was substituted with equivalent Na^+ , Fig. 4D and E. Here, menthol (100 μ M) rapidly increased both inward and outward currents. Repeated measurements showed that added menthol (100 μ M) increased slope conductance from control value of 0.291 ± 0.050 nS/pF to 0.711 ± 0.136 nS/pF with added menthol ($n = 17$; $p < 0.01$). 2-APB (100 μ M), Fig. 4F, inhibited the increase in membrane current by menthol to 0.249 ± 0.108 nS/pF ($n = 5$; $p < 0.05$). Moreover, we note that stimulation of membrane current by added menthol occurred in only 17 out of 53 measurements or 32% of cells.

Discussion

These results are consistent with menthol's action as a well-established agonist of TRPM8 ion channels, which function primarily as a cold/menthol receptor in sensory neurons [7,15,16]. Yet, TRPM8 was first cloned from human prostate tumor cells [6], where it appears to be diagnostic of androgen-dependent tumors [17]. However, it also serves to regulate intracellular Ca^{2+} and to maintain cell survival [8]. Now we show that human GBM cells contain TRPM8, where it plays a role in mechanisms controlling GBM cell migration.

TRPM8 in human GBM cells may serve as a locus for menthol-stimulated Ca^{2+} entry, because TRPM8 mRNA and protein are ex-

pressed in human DBTRG cells. Two proteins contain an epitope for the TRPM8 antibody. The faint 130–140 kDa band is consistent with the molecular weight of TRPM8 in situ [15,16]. The 95–100 kDa bands are more consistent with constitutive activity of TRPM8 in endoplasmic reticulum from expression of a truncated TRPM8 splice variant [14]. Our present findings cannot confirm two TRPM8 isoforms in DBTRG cells, because we have not sequenced the proteins found in the distinct bands. Yet, such interpretation is consistent with two proteins having a common epitope.

Menthol's effect to increase $[Ca^{2+}]_i$ was much greater among migrating cells compared with non-migrating cells. So, it is possible that only migrating cells express full-length protein within the plasma membrane. This may explain why some DBTRG cells did not respond to menthol. Further work is needed to establish differential expression of TRPM8 proteins, but it is noteworthy that confluent cultures of DBTRG cells were used for immunoblot studies with few, if any, migrating cells. Hence, the faint 130–140 kDa band may result from there being few, if any, migrating cells in confluent cultures.

Non-responsiveness to added menthol also may have resulted from rapid rundown of TRPM8 channel activity by pipette dialysis of key cellular regulators, such as phosphatidylinositol 4,5-bisphosphate [18,19]. However, it seems unlikely that this would occur only in some cells. Alternatively, menthol may increase $[Ca^{2+}]_i$ independently of TRPM8 by effecting Ca^{2+} release from an intracellular store as reported for various cells [9]. Again, this does not explain why a substantial proportion of DBTRG cells were unresponsive to added menthol, nor does it explain the different responses to menthol in migrating versus non-migrating cells. Menthol also has no effect on DBTRG cells free of external Ca^{2+} .

Menthol stimulates DBTRG cell migration comparable to that by added HGF/SF. HGF/SF also increases $[Ca^{2+}]_i$ in DBTRG cells. Comparable inhibitory effects of 2-APB on HGF/SF- and menthol-stimulated DBTRG cell migration suggests that TRPM8 may be involved in cellular mechanisms of migration common to both agents. However, the relative non-specificity of 2-APB tempers this conclusion. Still, it is well-established that both agonists increase $[Ca^{2+}]_i$ [9,20]. Clearly more work is needed to establish signaling pathways that may be common to both agonists; and also to identify an in situ ligand for the TRPM8 ion channel, since intracranial temperature seemingly does not vary. Phosphatidylinositol 4,5-bisphosphate (PIP₂) plays a central role in the activation of TRPM8 by either cold or menthol [18]. Others, recognizing the constant temperature of the prostate gland, have identified lysophospholipids from the phospholipase-A₂ cleavage of phosphatidylcholine as activators of TRPM8 [21,22]. Thus, it is of interest that lysophosphatidic acid, the end metabolite in this cascade, stimulates $[Ca^{2+}]_i$ and motility of GBM cells [23,24].

Menthol's stimulation of membrane current indicates expression of TRPM8 channels in DBTRG cells. However, we cannot explain the inwardly-rectifying current component. TRPM8 currents are predominantly outwardly-rectifying [13], although cooling shifts the voltage-dependent activation by menthol from depolarized potentials to those of the physiologic range [25]. Moreover, the potential for half maximal activation of TRPM8 by cold was ~140 mV more negative in native channels compared with recombinant channels [26]. It is possible that gating of TRPM8 may vary with the isoform in GBM cells compared with that in situ and in heterologous expression systems.

In summary, our present findings indicate that GBM cells express TRPM8 mRNA and protein. Moreover, added menthol, along with HGF/SF, increases $[Ca^{2+}]_i$ and cell migration. We conclude that TRPM8 mediates, in part, the action of menthol and HGF/SF to increase $[Ca^{2+}]_i$ and enhance tumor invasion.

References

- [1] J. Vriens, A. Janssens, J. Prenen, B. Nilius, R. Wondergem, TRPV channels and modulation by hepatocyte growth factor/scatter factor in human hepatoblastoma (HepG2) cells, *Cell Calcium* 36 (2004) 19–28.
- [2] J. Waning, J. Vriens, G. Owsianik, L. Stuwe, S. Mally, A. Fabian, C. Fripiat, B. Nilius, A. Schwab, A novel function of capsaicin-sensitive TRPV1 channels: involvement in cell migration, *Cell Calcium* 42 (2007) 17–25.
- [3] C. Birchmeier, W. Birchmeier, E. Gherardi, G.F. Vande Woude, Met, metastasis, motility and more, *Nat. Rev. Mol. Cell Biol.* 4 (2003) 915–925.
- [4] S. Koochekpour, M. Jeffers, S. Rulong, G. Taylor, E. Klineberg, E.A. Hudson, J.H. Resau, G.F. Vande Woude, Met and hepatocyte growth factor/scatter factor expression in human gliomas, *Cancer Res.* 57 (1997) 5391–5398.
- [5] J. Laterra, E. Rosen, M. Nam, S. Ranganathan, K. Fielding, P. Johnston, Scatter factor/hepatocyte growth factor expression enhances human glioblastoma tumorigenicity and growth, *Biochem. Biophys. Res. Commun.* 235 (1997) 743–747.
- [6] L. Tsavaler, M.H. Shaper, S. Morkowski, R. Laus, Trp-p8, a novel prostate-specific gene, is up-regulated in prostate cancer and other malignancies and shares high homology with transient receptor potential calcium channel proteins, *Cancer Res.* 61 (2001) 3760–3769.
- [7] D.M. Bautista, J. Siemens, J.M. Glazer, P.R. Tsuruda, A.I. Basbaum, C.L. Stucky, S.E. Jordt, D. Julius, The menthol receptor TRPM8 is the principal detector of environmental cold, *Nature* 448 (2007) 204–208.
- [8] L. Zhang, G.J. Barritt, Evidence that TRPM8 is an androgen-dependent Ca^{2+} channel required for the survival of prostate cancer cells, *Cancer Res.* 64 (2004) 8365–8373.
- [9] F. Mahieu, G. Owsianik, L. Verbert, A. Janssens, H. De Smedt, B. Nilius, T. Voets, TRPM8-independent menthol-induced Ca^{2+} release from endoplasmic reticulum and Golgi, *J. Biol. Chem.* 282 (2007) 3325–3336.
- [10] T.W. Ecay, T.D. Conner, E.R. Decker, Nonmuscle myosin IIA copurifies with chloride channel-enriched membranes from epithelia, *Biochem. Biophys. Res. Commun.* 231 (1997) 369–372.
- [11] T.W. Ecay, J.R. Stewart, D.G. Blackburn, Expression of calbindin-D28K by yolk sac and chorioallantoic membranes of the corn snake, *Elaphe guttata*, *J. Exp. Zool. B Mol. Dev. Evol.* 302 (2004) 517–525.
- [12] O.P. Hamill, A. Marty, E. Neher, B. Sakmann, F.J. Sigworth, Improved patch-clamp techniques for high-resolution current recording from cells and cell-free membrane patches, *Pflügers Arch.* 391 (1981) 85–100.
- [13] T. Voets, G. Owsianik, B. Nilius, Trpm8, *Handbook Exp. Pharmacol.* (2007) 329–344.
- [14] G. Bidaux, M. Flourakis, S. Thebault, A. Zholos, B. Beck, D. Gkika, M. Roudbaraki, J.L. Bonnal, B. Mauroy, Y. Shuba, R. Skryma, N. Prevarskaya, Prostate cell differentiation status determines transient receptor potential melastatin member 8 channel subcellular localization and function, *J. Clin. Invest.* 117 (2007) 1647–1657.
- [15] A.M. Peier, A. Moqrich, A.C. Hergarden, A.J. Reeve, D.A. Andersson, G.M. Story, T.J. Earley, I. Dragoni, P. McIntyre, S. Bevan, A. Patapoutian, A TRP channel that senses cold stimuli and menthol, *Cell* 108 (2002) 705–715.
- [16] D.D. McKemy, W.M. Neuhauser, D. Julius, Identification of a cold receptor reveals a general role for TRP channels in thermosensation, *Nature* 416 (2002) 52–58.
- [17] L. Zhang, G.J. Barritt, TRPM8 in prostate cancer cells: a potential diagnostic and prognostic marker with a secretory function?, *Endocr. Relat. Cancer* 13 (2006) 27–38.
- [18] B. Liu, F. Qin, Functional control of cold- and menthol-sensitive TRPM8 ion channels by phosphatidylinositol 4,5-bisphosphate, *J. Neurosci.* 25 (2005) 1674–1681.
- [19] T. Rohacs, C.M. Lopes, I. Michailidis, D.E. Logothetis, PI(4,5)P₂ regulates the activation and desensitization of TRPM8 channels through the TRP domain, *Nat. Neurosci.* 8 (2005) 626–634.
- [20] G. Baffy, L. Yang, G.K. Michalopoulos, J.R. Williamson, Hepatocyte growth factor induces calcium mobilization and inositol phosphate production in rat hepatocytes, *J. Cell. Physiol.* 153 (1992) 332–339.
- [21] D.A. Andersson, M. Nash, S. Bevan, Modulation of the cold-activated channel TRPM8 by lysophospholipids and polyunsaturated fatty acids, *J. Neurosci.* 27 (2007) 3347–3355.
- [22] F. Vanden Abeele, A. Zholos, G. Bidaux, Y. Shuba, S. Thebault, B. Beck, M. Flourakis, Y. Panchin, R. Skryma, N. Prevarskaya, Ca(2+)-independent phospholipase A(2)-dependent gating of TRPM8 by lysophospholipids, *J. Biol. Chem.* 281 (2006) 40174–40182.
- [23] Y. Kishi, S. Okudaira, M. Tanaka, K. Hama, D. Shida, J. Kitayama, T. Yamori, J. Aoki, T. Fujimaki, H. Arai, Autotaxin is overexpressed in glioblastoma multiforme and contributes to cell motility of glioblastoma by converting lysophosphatidylcholine to lysophosphatidic acid, *J. Biol. Chem.* 281 (2006) 17492–17500.
- [24] T.J. Manning Jr., J.C. Parker, H. Sontheimer, Role of lysophosphatidic acid and rho in glioma cell motility, *Cell Motil. Cytoskeleton* 45 (2000) 185–199.
- [25] T. Voets, G. Droogmans, U. Wissenbach, A. Janssens, V. Flockerzi, B. Nilius, The principle of temperature-dependent gating in cold- and heat-sensitive TRP channels, *Nature* 430 (2004) 748–754.
- [26] A. Malkia, R. Madrid, V. Meseguer, E. de la Pena, M. Valero, C. Belmonte, F. Viana, Bidirectional shifts of TRPM8 channel gating by temperature and chemical agents modulate the cold sensitivity of mammalian thermoreceptors, *J. Physiol.* 581 (2007) 155–174.